Epoxy−Silica Mesocomposites with Enhanced Tensile Properties and Oxygen Permeability

In Park,[†] Hua-gen Peng,[‡] David W. Gidley,[‡] Siqi Xue,[†] and Thomas J. Pinnavaia*[,†]

Department of Chemistry, Michigan State University, East Lansing, Michigan 48824, and Department of Physics, University of Michigan, Ann Arbor, Michigan 48109

Received August 8, 2005. Revised Manuscript Received November 30, 2005

As-made and calcined forms of large-pore (5.3 nm) mesostructured silica with a wormhole framework structure, denoted MSU-J, have been used to form rubbery epoxy mesocomposites containing 1.0−12% (w/w) silica. The tensile modulus, strength, toughness, and extension-at-break for the mesocomposites formed from as-made and calcined forms of MSU-J silica are systematically reinforced by up to 4.8, 5.7, 1.6, and 8.5 times, respectively, in comparison to the pure epoxy polymer. The composites represent the first examples wherein the reinforcement benefits provided by mesostructured silica particles are comparable to those provided by exfoliated organoclay nanolayers at equivalent loadings. Moreover, the reinforcement benefits are realized without the need for organic modification of the silica surface, and the increases in tensile properties occur with little or no sacrifice in optical transparency or thermal stability. The oxygen permeability of the mesocomposites prepared from as-made MSU-J silica increases dramatically at loadings ≥5.0% (w/w), whereas the compositions made from the calcined form of the mesostructure show no permeation dependence on silica loading. For instance, the oxygen permeability of the mesocomposites containing 12% (w/w) as-made MSU-J silica is 6-fold higher than that of the silica-free epoxy membrane. Positron annihilation lifetime spectroscopy established the absence of free volume in the mesocomposites, thus precluding the possibility of facile oxygen diffusion through the framework pores of the silica. The increase in oxygen permeability is correlated with the partitioning of curing agent between the as-made mesostructure and the liquid prepolymer, which leads to coronas of permeable polymer with reduced chain cross-linking in the vicinity of the silica particles. Mesocomposites made from calcined forms of the mesostructured silica do not allow for curing agent partitioning, and the oxygen permeability is not significantly influenced by the silica loading.

Introduction

Inorganic particles with a domain size less than 100 nm in at least one dimension can enhance the tensile properties of a polymer through beneficial interactions at the polymer−particle interface.[1] Layered silicate clays in exfoliated form have been widely investigated in recent years as reinforcing agents, as well as barrier and flame retardation agents, for a variety of organic polymer systems.[2−4] Unlike conventional composites formed from monolithic particles, clay nanocomposites are formed through the complete dispersion (exfoliation) of the nanolayers that comprise the clay tactoids. This exfoliation process provides a large surface area (∼750 m^2/g) and a high particle aspect ratio (≥200)[5] that normally cannot be achieved with monolithic particles.

Mesostructured silica and other metal oxides[6] represent another class of inorganic material that more recently has been considered for polymer composite formation. These solids have controllable nanopores (2−10 nm) and surface areas that are even higher than exfoliated clays, though the particle morphology tends to be isotropic. Mesostructured silica with a large mesopore size has shown promise for the formation of novel polymer composites.[7] For example, the one-dimensional channels of hexagonal MCM-41 have been used to direct the polymerization of conjugated polymers such as polydiacetylene,[8] polyvinylene,[9,10] and polythiophene.[11] The alignment of the polymers within the pores can result in unusual chromatic changes, polarized luminescence, and stability after multiple cyclovoltametric cycles. Nevertheless, there has been only a few attempts to improve the mechanical[12−14] and permeability properties[15] of a polymer using mesoporous silica as an adjuvant.

* To whom correspondence should be addressed. E-mail: pinnavai@cem.msu.edu.
† Michigan State University.
‡ University of Michigan.

(1) Novak, B. M. *Adv. Mater.* **1993**, *5*, 422.
(2) Giannelis, E. P. *Adv. Mater.* **1996**, *8*, 29.
(3) Kojima, Y.; Usuki, A.; Kawasumi, M.; Okada, A.; Fukushima, Y.; Kurauchi, T.; Kamigaito, O. *J. Mater. Res.* **1993**, *8*, 1185.
(4) Yano, K.; Usuki, A.; Okada, A.; Kurauchi, T.; Kamigaito, O. *J. Polym. Sci., Polym. Chem.* **1993**, *31*, 2493.
(5) LeBaron, P. C.; Wang, Z.; Pinnavaia, T. J. *Appl. Clay Sci.* **1999**, *15*, 11.
(6) Kresge, C. T.; Leonowicz, M. E.; Roth, W. J.; Vartuli, J. C.; Beck, J. S. *Nature* **1992**, *359*, 710.
(7) Shi, J. L.; Hua, Z. L.; Zhang, L. X. *J. Mater. Chem.* **2004**, *14*, 795.
(8) Lu, Y. F.; Yang, Y.; Sellinger, A.; Lu, M. C.; Huang, J. M.; Fan, H. Y.; Haddad, R.; Lopez, G.; Burns, A. R.; Sasaki, D. Y.; Shelnutt, J.; Brinker, C. J. *Nature* **2001**, *411*, 617.
(9) Nguyen, T. Q.; Wu, J. J.; Doan, V.; Schwartz, B. J.; Tolbert, S. H. *Science* **2000**, *288*, 652.
(10) Molenkamp, W. C.; Watanabe, M.; Miyata, H.; Tolbert, S. H. *J. Am. Chem. Soc.* **2004**, *126*, 4476.
(11) Li, G. T.; Bhosale, S.; Wang, T. Y.; Zhang, Y.; Zhu, H. S.; Fuhrhop, K. H. *Angew. Chem., Int. Ed.* **2003**, *42*, 3818.
(12) Kojima, Y.; Matsuoka, T.; Takahashi, H. *J. Appl. Polym. Sci.* **1999**, *74*, 3254.

10.1021/cm051768r CCC: $33.50
Published on Web 01/06/2006

Although embedded nanoparticles can improve both the barrier and the mechanical properties of a polymer for potential applications in packaging,[16] it generally is much more difficult to enhance the permeability of a polymer for gas separation applications without compromising polymer strength.[17] Porous zeolite molecular sieve and mesostructured silica particles have been shown to improve the permeability polymer-based membranes.[15,18−23] For example, the addition of 30% (w/w) MCM-41 to polysulfone boosts the oxygen permeability by 155% without a loss in O_2/N_2 selectivity due to increased diffusivity through nonselective voids.[15] However, the composite membranes became increasingly brittle with increasing mesostructured silica loading. Similar improvements in permeability at the expense of strength have been observed for amine-functionalized polyimide membranes[23] embedded with mesostructured silica.

We recently reported a large-pore mesostructured silica, denoted MSU-J,[24] assembled from tetraethyl orthosilicate as the silica source and the α,ω-diamine polypropylene oxide $H_2NCH(CH_3)CH_2[OCH_2CH(CH_3)]_xNH_2$ ($x = \sim 33$) as the structure-directing agent. The latter amine, which is commercially available under the trade name Jeffamine D2000, also has been used as a cross-linking agent[25−27] for the formation of rubbery epoxy polymers. In the present study we investigate the properties of as-made, amine-intercalated MSU-J mesostructured silica for the synthesis of epoxy−silica mesocomposites. For comparison purposes we also have used the surfactant-free calcined version of MSU-J silica for epoxy composite formation. The three-dimensional wormhole[28,29] pore network (average pore size 5.3 nm) and the high surface area (~950 m^2/g) of MSU-J silica is shown to substantially improve the tensile properties of the polymer. Also, we report the unexpected enhancement in the oxygen permeation properties for composite compositions derived from as-made MSU-J mesostructures. The observed enhancement in oxygen permeability may find use for the design of composite membranes based on mesostructured forms of silica.

Experimental Section

Materials. Epoxy resin EPON 828, a diglycidyl ether of bisphenol (Resolution Performance Products, $M_w \sim 377$), was used for the preparation of epoxy−MSU-J silica mesocomposites. The α,ω-diamine-functionalized polypropylene oxide $H_2NCH(CH_3)CH_2[OCH_2CH(CH_3)]_xNH_2$ ($x = \sim 33$) with an average molecular weight of ~2000 was obtained from Hintsman Chemical Co. under the trade name Jeffamine D2000. The amine was used both as an epoxy curing agent and as a structure-directing agent for the synthesis of MSU-J silica. Sodium silicate (27% SiO_2, 14% NaOH solution) was purchased from Aldrich and used as a silica precursor for the preparation of MSU-J mesostructured silica.

Synthesis of Mesostructured MSU-J Silica. The Jeffamine D2000 porogen was mixed with an amount of aqueous HCl solution equivalent to the hydroxide content of the sodium silicate solution. The silica source was added to the porogen solution under vigorous stirring at ambient temperature and the mixture was allowed to age at 25 °C for 20 h. The optimum molar composition for the formation of as-made MSU-J was 1.0:0.83:0.125:0.83:230 SiO_2:NaOH:Jeffamine D2000:HCl:H_2O. The porogen-intercalated as-made mesostructured product, denoted as-made MSU-J, was recovered by filtration and dried in air at ambient temperature. A porogen-free analogue of the mesostructure, denoted calcined MSU-J, was obtained by calcination of as-made MSU-J at 600 °C for 4 h. The as-made and calcined forms of the mesostructures were ground to a powder for future use.

Preparation of Epoxy−MSU-J Silica Mesocomposites. A predetermined amount of as-made or calcined MSU-J silica was added to the epoxy resin and mixed at 50 °C for 10 min. The amount of Jeffamine D2000 curing agent needed to achieve an overall NH:epoxide stoichiometry of 1:1 was then added to the mixture and mixed at 50 °C for another 10 min. For composites prepared from the as-made mesostructure, the Jeffamine D2000 present in the pores of the mesostructure was counted as contributing to the curing process. The resulting suspensions were outgassed under vacuum and transferred to an aluminum mold. Pre-curing of the nanocomposite was carried out under nitrogen gas flow at 75 °C for 3 h, followed by an additional 3 h cure at 125 °C to complete the cross-linking.

To compare the optical transparency of an epoxy−as-made MSU-J mesocomposite against a conventional epoxy−epoxy nanocomposite, an octadecylammonium-modified montmorillonite (ODA-MMT, Nanocor Inc.) was used as a reinforcing agent. Approximately 65% of the cation exchange sites of the ODA-MMT clay are occupied by ODA cations and the remaining sites are occupied by protons. A procedure analogous to that used to prepare the as-made MSU-J−epoxy mesocomposites was used to prepare the clay composites.

Physical Measurements. X-ray diffraction (XRD) patterns were obtained on a Rigaku Rotaflex 200B diffractometer equipped with Cu Kα X-ray radiation and a curved crystal graphite monochromator operating. Samples of the liquid epoxy−silica mixture were prepared by pouring the suspension onto filter paper mounted on a glass slide and blotting away the excess liquid. Cured nanocomposites were examined by mounting a rectangular flat specimen into an aluminum X-ray sample holder. XRD patterns with equivalent intensities were obtained for the upper and lower surfaces of the cured mesocomposites containing 12 wt % silica, thus verifying the uniform dispersion of mesostructured silica in the epoxy matrix.

Transmission electron microscopy (TEM) images were taken on a JEOL JEM-100CX II microscope with a CeB_6 filament and an

(13) Ji, X. L.; Hampsey, J. E.; Hu, Q. Y.; He, J. B.; Yang, Z. Z.; Lu, Y. F. *Chem. Mater.* **2003**, *15*, 3656.
(14) He, J.; Shen, Y. B.; Yang, J.; Evans, D. G.; Duan, X. *Chem. Mater.* **2003**, *15*, 3894.
(15) Reid, B. D.; Ruiz-Trevino, A.; Musselman, I. H.; Balkus, K. J.; Ferraris, J. P. *Chem. Mater.* **2001**, *13*, 2366.
(16) Pinnavaia, T. J.; Beall, G. W. *Polymer-Clay Nanocomposites*; John Wiley and Sons: New York, 2001.
(17) Maier, G. *Angew. Chem., Int. Ed.* **1998**, *37*, 2961.
(18) Kulprathipanja, S.; Neuzil, R. W.; Li, N. N. Separation of Fluids by Means of Mixed Matrix Membranes. U.S. Patent 4,740,219, 1988.
(19) Jia, M. D.; Peinemann, K. V.; Behling, R. D. *J. Membr. Sci.* **1991**, *57*, 289.
(20) Duval, J. M.; Folkers, B.; Mulder, M. H. V.; Desgrandchamps, G.; Smolders, C. A. *J. Membr. Sci.* **1993**, *80*, 189.
(21) Gur, T. M. *J. Membr. Sci.* **1994**, *93*, 283.
(22) Suer, M. G.; Bac, N.; Yilmaz, L. *J. Membr. Sci.* **1994**, *91*, 77.
(23) Balkus, K. J.; Cattanach, K.; Musselman, I. H.; Ferraris, J. P. *Mater. Res. Soc. Symp. Proc.* **2003**, *752*, 91.
(24) Park, I.; Wang, Z.; Pinnavaia, T. J. *Chem. Mater.* **2005**, *17*, 383.
(25) Triantafillidis, C. S.; LeBaron, P. C.; Pinnavaia, T. J. *Chem. Mater.* **2002**, *14*, 4088.
(26) Shan, L.; Verghese, K. N. E.; Robertson, C. G.; Reifsnider, K. L. *J. Polym. Sci., Polym. Phys.* **1999**, *37*, 2815.
(27) Liang, W. J.; Kao, H. M.; Kuo, P. L. *Macromol. Chem. Phys.* **2004**, *205*, 600.
(28) Lee, J.; Yoon, S.; Oh, S. M.; Shin, C. H.; Hyeon, T. *Adv. Mater.* **2000**, *12*, 359.
(29) Lee, J.; Han, S.; Hyeon, T. *J. Mater. Chem.* **2004**, *14*, 478.

accelerating voltage of 120 kV. Sample grids of calcined mesoporous silicas were prepared via sonication of a powdered sample in ethanol for 10 min and evaporation of 2 drops of the suspension onto a holey carbon film supported on a 3 mm, 300 mesh copper grid. Thin-sectioned samples were obtained by embedding the rubbery nanocomposite flakes in a glassy epoxy matrix and sectioning on an ultramicrotome.

Tensile measurements on individually molded samples were performed at ambient temperature according to ASTM standard D3039 using an SFM-20 United Testing System. The dog-bone-shaped specimens used in the tensile testing were 28 mm long in the narrow region, 3 mm thick, and 3 mm wide along the center of the casting. At least four stress−strain data points with good precision were obtained and the results averaged. For a typical instance, the errors in modulus and strength for the composites containing 12% (w/w) as-made MSU-J silica are ±1.2 and ±0.50, respectively, based on the 95% confidence interval for the mean values.

Oxygen permeability data were recorded on a MOCON Oxtran 2/60 oxygen permeability instrument with a test gas containing 100% oxygen, nitrogen (containing 2 vol % hydrogen) as a carrier gas. Film samples with a thickness between 0.9 and 1.5 mm, area of 0.317 cm^2, were cast from an aluminum disk mold and were loaded in the testing cells with adhesive aluminum foil masks.

Thermogravimetric analyses (TGA) were performed using a computer-controlled Shimadzu TGA-50 thermal analyzer. Typically, a 50-mg sample was placed in a Pyrex bucket and heated at ambient temperature to 800 °C at a rate of 5 °C/min in a nitrogen flow of 50 mL/min.

Positronium Annihilation Lifetime Spectroscopy (PALS) was performed with a standard fast timing spectrometer with a 0.30 ns time resolution. A ^{22}Na source that emits about 10^6 positrons/s is sealed between two thin sheets of Ni foil and then sandwiched between two identical sheets (each sheet is about 2 cm square) of the sample to be studied. Positrons are emitted from the source simultaneously with a 1270 keV gamma ray (detected as the "start" signal) and some 80% penetrate the sealing foil and stop in the target sample. About 30% of the positrons stopping in the neat epoxy form positronium, the bound state of the positron and electron, which tends to localize in free volume voids. Subsequent annihilation of the positronium produces 511 keV radiation detected as the "stop" signal and the time between each start and stop signal pair is recorded as a time histogram. This lifetime spectrum is fitted for exponential lifetime components wherein the lifetime and intensity are related to void size and porosity.

Results

A large-pore mesostructured silica with a wormhole framework structure, denoted MSU-J, was assembled from sodium silicate and Jeffamine D2000 as the structure-directing porogen according to previously described methods.[24] The pore diameter (5.3 nm), pore volume (1.41 cm^3/g), and surface area (947 m^2/g) were determined by a N_2 adsorption isotherm following calcination of the as-made mesostructure at 600 °C. It is presumed that the as-made mesostructure, which contains 58% (w/w) Jeffamine D2000 porogen in the framework mesopores, has similar textural properties.

Both the as-made and the calcined forms of the mesostructure were used in forming rubbery epoxy mesocomposites. The mesocomposites formed from as-made MSU-J have the Jeffamine D2000 curing agent initially partitioned between the silica mesophase and the pre-polymer resin. For the mesocomposites formed from the porogen-free calcined form of MSU-J, however, all the curing agent is contained initially in the bulk pre-polymer prior to the curing reaction.

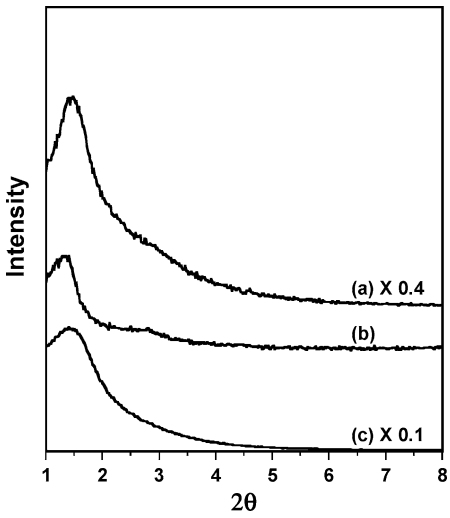

Figure 1. Small-angle powder X-ray diffraction patterns: (a) as-made MSU-J mesostructure containing 58% (w/w) intercalated Jeffamine D2000; (b) epoxy−silica mesocomposite (12 wt % silica) formed from as-made MSU-J; (c) mesostructured silica recovered through calcination at 600 °C of a mesocomposite containing 12% (w/w) silica.

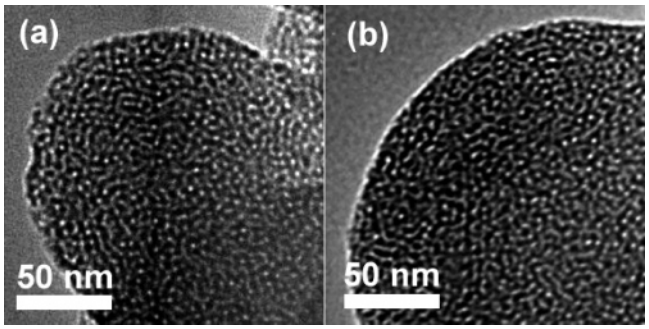

Figure 2. TEM images of (a) calcined MSU-J silica and (b) the silica obtained through calcination at 600 °C a cured epoxy−silica mesocomposite (12 wt % silica) formed from as-made MSU-J silica.

Figure 1 compares the small-angle XRD patterns for the as-made MSU-J mesostructure (curve a) with the pattern of the mesostructure dispersed at the 12% (w/w) level in a cured epoxy composite (curve b). The presence of a low-angle reflection, corresponding to a *d* spacing of 6.0 nm, is indicative of the average pore−pore correlation distance for a wormhole framework. The wormhole framework structure is verified by the TEM shown in Figure 2a. The loss of diffraction intensity upon dispersion of the mesostructure in the cured composite is attributable to contrast matching between the silica walls and cured polymer formed in the mesopores. Evidence supporting the contrast matching effect is provided by the increase in intensity observed upon removal of the polymer through calcination (curve c). Analogous XRD scattering behavior was observed for the calcined MSU-J−epoxy composite system. These XRD data, along with the TEM image of Figure 2b of the recovered mesostructure, clearly show that the wormhole framework structure of MSU-J is retained in an epoxy matrix upon cross-linking at 125 °C.

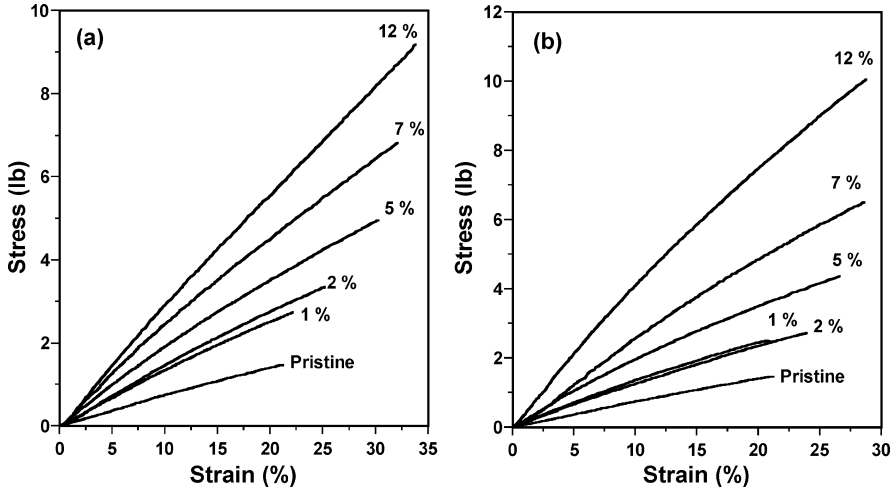

Figure 3. Comparison of stress−strain curves for pristine epoxy and MSU-J/epoxy mesocomposites containing different loadings of (a) as-made MSU-J silica and (b) calcined MSU-J silica.

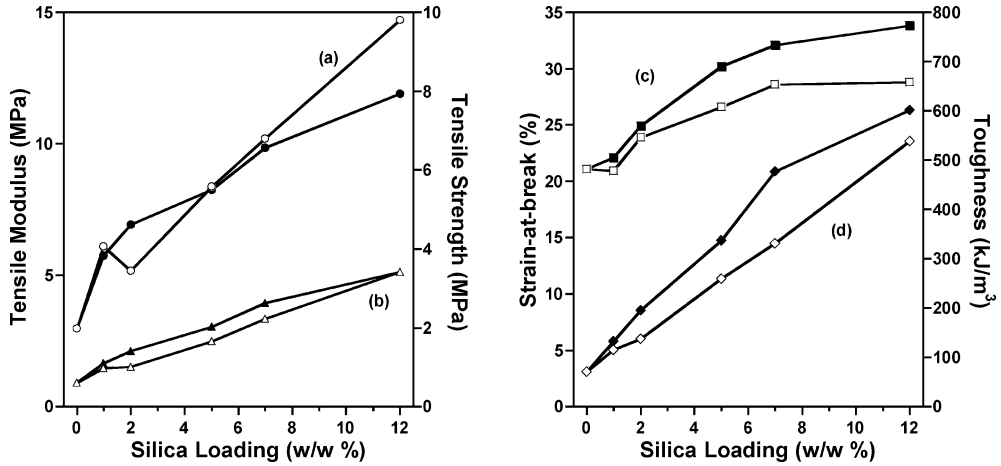

Figure 4. Loading dependence of the (a) tensile moduli, (b) tensile strengths, (c) strain-at-break, and (d) toughness for epoxy mesocomposites prepared from MSU-J silica. The solid and open data points are for the composites prepared from as-made and calcined MSU-J silica, respectively.

Tensile data were obtained from dog-bone-shaped specimens containing 1.0−12 wt % as-made and calcined MSU-J silica. A comparison of stress−strain curves as a function of silica loadings for the rubbery epoxy mesocomposites is provided in Figure 3. Both forms of the mesostructure provide composites with improved mechanical performance. The modulus, strength, elongation, and toughness of the epoxy composites prepared from the as-made and calcined forms of the silica generally increase with increasing silica loadings (Figure 4). Table 1 summarizes the values of tensile properties obtained at different silica loadings. Note that the composites formed from the as-made silica have a higher elongation-at-break so that the toughness of the composites increases more rapidly with increasing silica loading in comparison to the composites formed from calcined MSU-J.

The most significant difference in the properties of the mesocomposites formed from as-made and calcined MSU-J silica is observed in the oxygen permeability profiles of the composites. Figure 5 presents the O_2 permeability of the rubbery epoxy composites as a function of as-made and calcined MSU-J silica loadings. The oxygen permeability for the nanocomposites prepared from the calcined mesostructure is nearly independent of the silica content of the epoxy matrix over the entire loading range 0−12% (w/w) silica. The as-made MSU-J system, in contrast, shows behavior similar to the calcined silica composites only at low silica loadings (1−3 wt %). An abrupt and significant increase in oxygen permeability occurs at 5 wt % loading. Relative to the pristine polymer, a 5- to 6-fold increase in oxygen permeability is observed over the silica loading range 7−12% (w/w). Oxygen permeability increases of this magnitude are unprecedented among polymer-based nanocomposites containing dispersed porous particulates.

PALS results for the neat epoxy and two samples of the as-made MSU-J silica composites (2% and 10% w/w) are quite definitive. The neat epoxy displays a very typical 2.7 ns positronium lifetime (with a relative intensity of 20%) that corresponds to 0.7 nm diameter voids inherent to the material. The two spectra from the MSU-J silica composites are almost identical except that the 10% w/w film has a relative intensity of the 2.7 ns lifetime of only 18%. The 10% drop in relative intensity corresponds to the 10% of positrons that stop in the silica phase which does not have a 2.7 ns lifetime. There is no indication of any longer positronium lifetimes as would be expected if the silica pores where vacant (5 nm pores would correspond to lifetimes in the 50−80 ns range). Special long time-range PALS runs with high sensitivity to such long lifetimes were performed and an *upper limit* of 0.15% relative intensity could be set on any such components (i.e., less than 1% of the 20%

Table 1. Tensile, Thermal Stability, and Oxygen Permeability Properties of Pristine Epoxy Polymer and Epoxy/MSU-J Mesocomposites

sample	silica loading (w/w %)	tensile modulus (MPa)	tensile strength (MPa)	elongation (%)	toughness (kJ m^{-3})	thermal stability[a] (°C)	oxygen permeability ($cm^3 \cdot mil \cdot m^{-2} \cdot day^{-1}/10^4$)[b]
pristine polymer	0	2.96	0.60	21.1	71	269	2.3
as-made MSU-J mesocomposites	1	5.74	1.10	22.1	132		2.4
	2	6.93	1.40	24.9	195		2.3
	3						2.2
	5	8.24	2.02	30.2	337		9.3
	7	9.84	2.63	32.1	477		12
	10						12
	12	11.9	3.41	33.8	601	320	14
calcined MSU-J mesocomposites	1	6.09	0.98	20.9	115		2.8
	2	5.17	1.01	25.9	137		2.8
	3						2.4
	5	8.37	1.66	29.5	259		2.8
	7	10.2	2.23	28.8	331		2.6
	10						3.0
	12	14.7	3.42	29.9	539		2.0

[a] Temperature needed to achieve a weight loss of 1.5% (w/w). [b] A material with an oxygen permeability of 1 $cm^3 \cdot mil \cdot m^{-2} \cdot day^{-1}$ means that 1 cm^3 of oxygen will pass through a membrane of the material with a thickness of 1 mil (one-thousandth of inch) and an area of 1 m^2 over a period of 1 day.

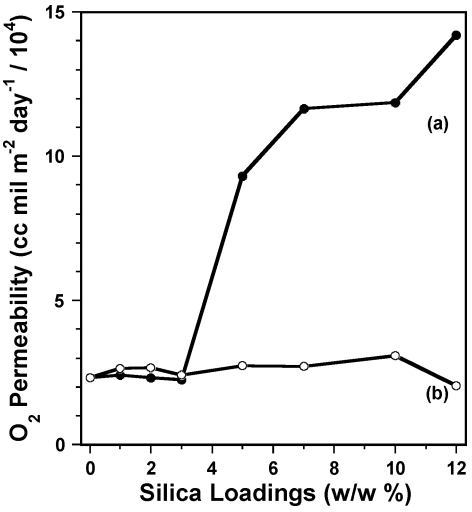

Figure 5. Dependence of oxygen permeability on silica loadings for epoxy mesocomposites prepared from (a) as-made MSU-J silica and (b) calcined MSU-J silica.

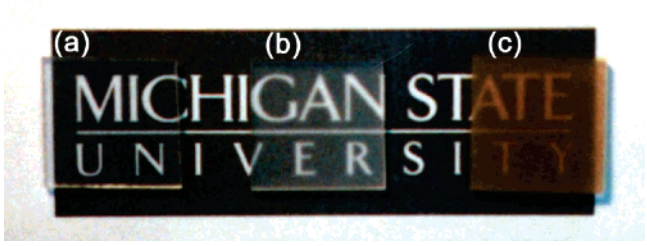

Figure 6. Optical image illustrating differences in the transparency of (a) pristine epoxy polymer and epoxy composites prepared from (b) as-made MSU-J silica at 10% (w/w) loading and (c) octadecylammonium-modified montmorillonite (ODA-MMT) at 10% (w/w) silicate loading.

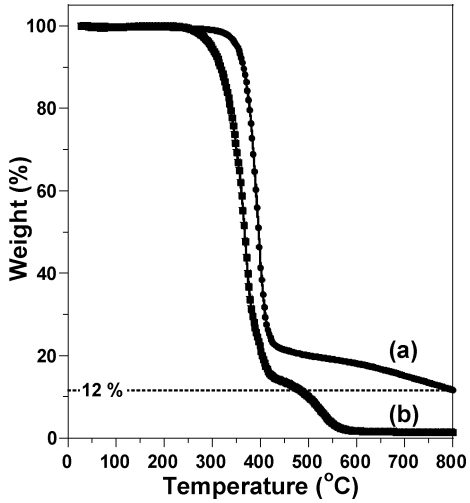

Figure 7. Thermogravimetric analysis curves in air for (a) the epoxy mesocomposite prepared from as-made MSU-J silica at a loading of 12% (w/w) silica and (b) the pristine epoxy polymer.

positronium intensity measured in the neat epoxy). Heating in a vacuum to 150 °C to drive off any absorbed water from environmental exposure yielded identical spectra. The PALS data are completely consistent with no voids in the as-made MSU-J silica mesocomposites, other than those microvoids inherent to the cured epoxy. The silica pores are fully occupied by cured polymer.

Another significant result derived from the epoxy−MSU-J mesocomposite systems relative to natural epoxy clay nanocomposites is the optical transparency of the mesocomposites. Figure 6 illustrates that the mesocomposite containing 10% (w/w) as-made MSU-J silica is substantially more transparent than an ODA-MMT composite containing the same loading of montmorillonite clay. The mesocomposites made from calcined MSU-J have a similar transparency. Thus, in comparison to clay nanoparticles, the refraction index of the MSU-J silica more nearly matches that of the epoxy matrix.

The thermal stability of the mesocomposites formed from as-made MSU-J is enhanced in comparison to the pristine polymer. As illustrated in Figure 7, the temperature needed to achieve a weight loss of 1.5% is increased by 50 °C relative to the pristine epoxy polymer. Along with the delayed first degradation stage, the maximum degradation rate is shifted from 365 °C for the pristine epoxy to 396 °C for the mesocomposite containing 12% (w/w) as-made MSU-J silica, as determined from the first derivative of the TGA curves. Additionally, the charring processes, which start at approximately 400 °C in both cases, is extended up to 800 °C for the as-made MSU-J composite at a 12% (w/w) loading.

Discussion

The XRD and TEM results shown in Figures 1 and 2 clearly establish retention of the mesophase phase structure upon dispersal of as-made and calcined MSU-J silica in a cured epoxy matrix. Little or no settling of the mesophase was observed during the polymer curing process because the intensity of the Bragg reflections from the upper and lower surfaces of the cured composite specimens were equivalent over the entire range of silica loadings.

The substantial improvements in the modulus, strength, and toughness achieved for the MSU-J mesocomposites in comparison to those of the pristine polymer (cf. Table 1) most likely are a consequence of strong interfacial interactions and adhesion between the epoxy matrix and silica mesophase. It is important to note that favorable interfacial interactions are realized in these mesocomposites without the need for organic modification of the silica surface. The high surface area of the MSU-J silica (~950 m^2/g) facilitates such interfacial interactions. Similar improvements in tensile moduli, strengths, and strain-at-breaks have been observed for rubbery epoxy−organoclay nanocomposites.[30−32] The 4- to 5.5-fold increase in modulus at 12% (w/w) MSU-J loading is comparable to the 6-fold benefit in modulus provided by organoclay nanoparticles at an equivalent loading. Moreover, the benefit in tensile properties occurs with little or no sacrifice in transparency (cf. Figure 6) or thermal stability properties (cf. Figure 7).

In the case of exfoliated clay nanocomposites, the anisotropic clay platelets in the cured matrix can be partially aligned in the direction of the stress and further enhance the tensile properties.[30] This strain-induced alignment of particles is less significant for the more isotropic MSU-J silica particles. Differences in particle morphology and alignment under applied stress may be the reason the elongation-at-break is limited to 34% for the mesocomposites formed from as-made MSU-J, whereas for nanocomposites formed from exfoliated clay platelets the elongation-at-break is 50% at the same 12% (w/w) loading.[30] In any case, unlike conventional reinforced composites which sacrifice elasticity and toughness in exchange for benefits in modulus and strength,[32−34] mesostructured silica and exfoliated clay are unique in providing substantially improved tensile properties at relatively low particulate loadings.

We note that previous attempts to use three-dimensional mesostructured silica as a polymer reinforcing agent have not demonstrated mechanical improvements comparable to those achieved with exfoliated organoclays. For instance, Nylon 66 composites containing 35% (w/w) of a mesostructured silica denoted FSM[12] exhibited only a 2-fold increase in modulus. A mesostructured organosilica[13] and a silylated cubic MCM-48[14] mesostructure have been used as reinforcing agents for poly((3-trimethoxysilyl)propyl methacrylate) and poly(vinyl acetate), respectively. The latter composites exhibited improvements in tensile strength and modulus, but the elongation-at-break was sacrificed despite efforts to achieve compatible particle−polymer interfaces through extensive organic modification of the silica surface.

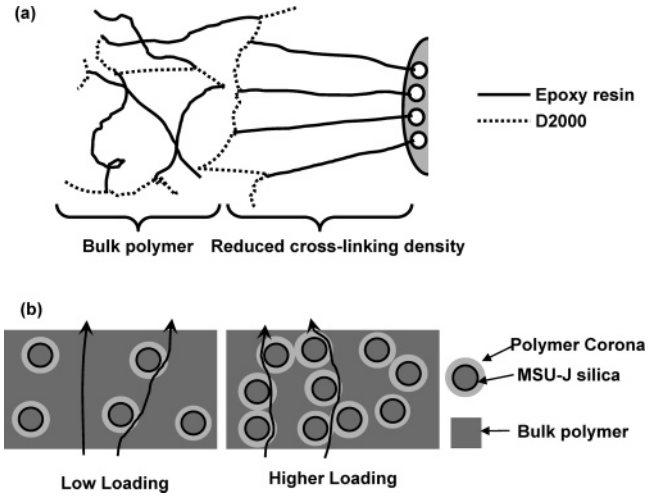

Figure 8. Schematic representations of (a) the proposed decrease in chain cross-linking density around the as-made MSU-J silica particles and (b) the proposed permeant gas pathways below and above ~5% (w/w) loading of as-made MSU-J silica.

The oxygen permeabilities of the mesocomposites formed from calcined MSU-J silica is independent of the particulate loading up to 12% (w/w) loading, as expected for a uniform dispersion of more or less isotropic particles in the polymer matrix (cf. Figure 5, curve (b)). However, the composite formed from as-made MSU-J silica shows an enhancement in oxygen permeability at a silica loading ≥5% (w/w) silica (cf. Figure 5, curve (a)). Both composite systems show no evidence for the presence of free volume, as judged by PALS. That is, the mesopores of the embedded silica in both mesocomposite systems are fully occupied by cured polymer. Thus, the enhancement in oxygen permeability for the mesocomposites made from as-made MSU-J silica cannot be attributed to diffusion through vacant pores in the mesostructured silica.

The main difference between the composites formed from as-made and calcined MSU-J silica lies in the initial distribution of the amine curing agent at the initial stages of the polymerization process. For as-made MSU-J, the amine is partitioned between the mesopores and the bulk resin, whereas for the calcined silica, the curing agent initially resides exclusively in the resin. The latter distribution of curing agent should lead to a uniform chain cross-linking throughout the polymer matrix. Although protonated amines act as an acid catalyst for epoxy-amine polymerization in the gallery regions of clays,[35] the silica−intercalated amine in as-made MSU-J is electrically neutral[36] and acid catalysis is not anticipated. However, the partitioning of the curing agent between the silica phase and the bulk pre-polymer may affect the rates for diffusion of resin and curing agent in to and out of the pores and lead to nonuniform chain cross-linking, particularly in the silica−polymer interface region.[37−39]

(30) Lan, T.; Pinnavaia, T. J. *Chem. Mater.* **1994**, *6*, 2216.
(31) Shi, H. Z.; Lan, T.; Pinnavaia, T. J. *Chem. Mater.* **1996**, *8*, 1584.
(32) Wang, Z.; Pinnavaia, T. J. *Chem. Mater.* **1998**, *10*, 1820.
(33) LeBaron, P. C.; Pinnavaia, T. J. *Chem. Mater.* **2001**, *13*, 3760.
(34) Ahmad, Z.; Sarwar, M. I.; Wang, S.; Mark, J. E. *Polymer* **1997**, *38*, 4523.
(35) Lan, T.; Kaviratna, P. D.; Pinnavaia, T. J. *Chem. Mater.* **1995**, *7*, 2144.
(36) Only 4 mol % of NH_2 groups of the D2000 (0.06M, $pK_b \sim 4$) are protonated in aqueous solution before the addition of the silica source.

As illustrated in Figure 8, a decrease in chain cross-linking near the silica interface would provide a corona of more permeable polymer around the silica particles and provide a percolation pathway for enhanced oxygen permeation. This proposed decrease in chain cross-linking density and concomitant increase in polymer flexibility in the interface region may also help explain why the mesocomposites prepared from as-made MSU-J silica are notably tougher than those prepared from the calcined form of the mesostructure (cf. Table 1).

We note that zeolite-loaded polymer membranes[19,21,22] have been reported wherein the oxygen permeability increases via a percolation pathway at a loading of ~30% (w/w).[22] For such membranes the zeolite pores are too small (<1 nm) to be filled by polymer and the permeant traverses the 0.30 cm^3/g void volume of the zeolite at the percolation threshold. The small pore sizes and hydrophilic surface cause poor interaction with the polymer chains, resulting in inadequate zeolite particle dispersion.[40,41] The deteriorated mechanical properties of zeolite−epoxy composites[41] substantiate zeolite de-wetting by the polymer chains. Due to the poor zeolite particle dispersion, nonselective zeolite voids cannot provide a facilitated diffusion pathway for the entire membrane in the diffusion direction until the zeolite loading reaches a very high value (~30 wt %). In the present work, the pore size (5.3 nm) and pore volume (1.41 cm^3/g) of the inorganic phase are much larger than a zeolite, and consequently, the pores are filled with polymer. The high level of as-made MSU-J particle dispersion and the formation of a permeable polymer corona around the particles provides for a permeation pathway at a relatively low particle loading of 5% (w/w). Modeling efforts will be needed to better estimate the corona size.

Acknowledgment. The support of this research by a NSF grant CHE-0211029 and NASA grant NAG3-2472 is gratefully acknowledged. The PALS work has been supported by a NSF grant ECS-0100009.

CM051768R

(37) Wind, J. D.; Staudt-Bickel, C.; Paul, D. R.; Koros, W. J. *Macromolecules* **2003**, *36*, 1882.
(38) Chung, T. S.; Chng, M. L.; Pramoda, K. P.; Xiao, Y. C. *Langmuir* **2004**, *20*, 2966.
(39) Robinson, J. P.; Tarleton, E. S.; Ebert, K.; Millington, C. R.; Nijmeijer, A. *Ind. Eng. Chem. Res.* **2005**, *44*, 3238.
(40) Zimmerman, C. M.; Singh, A.; Koros, W. J. *J. Membr. Sci.* **1997**, *137*, 145.
(41) Merkel, T. C.; Freeman, B. D.; Spontak, R. J.; He, Z.; Pinnau, I.; Meakin, P.; Hill, A. J. *Chem. Mater.* **2003**, *15*, 109.